



Research Article

Comparative synthesis of ZnO nanorods and nanoflowers as photocatalysts for the photodegradation of 4-chlorophenol

¹Manriquez Ramirez ME, ¹Wang JA, ²Gómez Romero JR, ¹Reza San Germán CM, ³Hernandez Cortez JG, ¹Zuniga Moreno A and ^{1,4}Estrada Flores M

¹Escuela Superior de Ingeniería Química e Industriales Extractivas, Instituto Politécnico Nacional, UPALM, Col. Zacatenco, 07738 México D.F., Mexico.

²Depto. Química, Universidad Autónoma Metropolitana-Iztapalapa, San Rafael Atlixco 186, 09340 México D.F. Mexico

³Programa de Ingeniería Molecular, Instituto Mexicano del Petróleo, Eje Central Lázaro Cárdenas 152, A.P. 14-805, 07730 México, D.F., Mexico.

⁴Instituto de Investigaciones en Materiales, Circuito Exterior S/N, Zona de Institutos, Ciudad Universitaria, C.P. 04510, México, D.F.

*Corresponding author E-mail: mestrada7@hotmail.com

Accepted 12 October 2014

Abstract

Nanostructured ZnO materials were comparatively synthesized via three different methods: precipitation, ultraviolet irradiation, and hydrothermal synthesis. ZnO with different morphologies such as flower-like and rods were obtained, depending on the synthetic method. XRD analysis indicates that ZnO single-crystallite particularly grows along the [002] direction in all samples. The photocatalytic activity in the photodegradation of 4-chlorophenol appears to be correlated with the surface oxygen deficiency, the band gap energy, and the morphologies of the samples. ZnO nanorods prepared by the precipitation method show higher activity in comparison with that achieved by the samples synthesized by ultraviolet irradiation and hydrothermal methods; in the latter shows higher band energy and there exists a great extent of lattice oxygen deficiency in the surface that is unfavorable in the formation of surface active oxygen species like superoxide radicals, thus exhibiting the lower photoactivity.

Keywords: ZnO synthesis, photoactivity, 4-chlorophenol, surface oxygen deficiency.

INTRODUCTION

ZnO is a semiconductor with a wide applications in the fields of blue/UV optoelectronics, transparent electronics, spintronic devices and sensors (Bunn, 2010; Tsukazaki et al., 2005; Dulub et al., 2002; Phillips, 1973). The polycrystalline form of ZnO is commonly used for producing facial powders, ointments, sunscreens, lubricant additives, piezoelectric transducers, varistors, and transparent conducting electrodes (Lide, 2005; Yong et al., 2007; Soltani et al., 2011; Gerward, 1995). Prospective photo-applications have revived interest in ZnO since it has direct band gap energy of 3.37 eV, which makes it excitable with UV radiation in blue wavelengths. The excitation binding energy is approximately 60 meV for ZnO; this high excitation binding energy enhances the luminescence efficiency of light emission (Kogure et al., 1998; Almamun et al., 2000, Liewhiran, 2007; Bates et al., 1962). It is well known that ZnO has hexagonal wurtzite crystalline structure in which Zn atoms are tetrahedrally coordinated with four O atoms, where the *d*-electrons hybridize with the O *p*-electrons. The bonding between the Zn atoms and O atoms is highly ionic, due to the

large difference in their electronegative values (1.65 for Zn and 3.44 for O). Alternating Zn and O layers form the crystal structure and ZnO can therefore be used as a UV-sensitive and solar-blind photodetector and transparent thin-film transistors (Özgür et al., 2005; Jagannatha et al., 2011; Agashe et al., 2010; Sharma et al., 2010). Some of the field-effect transistors even use ZnO nanorods as conducting channels (Look et al., 1999; Gorn et al., 2006). ZnO oxide used as photocatalyst for the degradation of organic compounds in polluted water is also reported (Qamar, 2009; Dunliang et al., 2009).

To improve the photoactivity of ZnO, a number of doped or mixed ZnO oxides have been synthesized by a wide range of methods, some of them expensive (Suzan, 2012). In recent years, a variety of ZnO nanostructure like nano-wires, nano-belts, nano-rods, nano-combs, nano-rings, etc. have been synthesized by some high temperature or high pressure processes (Maolin, 2005). However, less attention has been paid to the synthesis of ZnO using simple and inexpensive methods. In addition, different morphologies of nanostructural materials exhibit unique physical-chemical properties, therefore, control of size and morphology of ZnO crystals has attracted a great deal of interests. In the present work, synthesis of ZnO with nanorods and flower-like morphologies using several simple and inexpensive methods is reported. The photodegradation of 4-chlorophenol in water using ZnO solids was comparatively evaluated to study the morphology or surface structure-dependent photocatalytic performance of the samples. It is found that the photocatalytic activities are to be associated with the oxygen deficiency in the surface and the Zn-O band gap energy.

Experimental

Synthesis of ZnO nanostructures

ZnCl₂·6H₂O reagent grade obtained from Baker with a purity of 99.99 % was used to synthesize ZnO. All remaining chemicals were analytical grade without any further purification. Three different methods were used for obtaining ZnO nanostructures: precipitation, UV irradiation and hydrothermal synthesis.

Precipitation method

ZnO was synthesized by the precipitation method using 200 ml of a 0.25 M solution of NaOH to which ZnCl₂·6H₂O (20g) was added at 80 °C under constant stirring. Afterwards, the mixture was held for precipitation at 80 °C for 2 h. The precipitate was filtered, washed, and dried at 25 °C. Finally it was calcined at 400 °C in a muffle furnace for 12 h.

UV irradiation method

ZnCl₂·6H₂O (20g) was added to 200 ml of 0.25 M NaOH solution. The temperature was increased up to 80 °C with continuous stirring and held for a period of 5 hours under irradiation using a UV lamp. The resulting precipitate was collected by filtration, washed with water, and finally calcined at 400 °C in a muffle furnace for 12 h.

Hydrothermal method

ZnCl₂·6H₂O (20 g) was dissolved in a NaOH solution (60 ml 0.25M) under constant stirring for 10 min. The mixed dissolution was transferred into a PTFE-lined stainless steel autoclave (at 80% of a total 100 ml capacity). The autoclave was sealed and maintained at 90 °C for 5 h. After the reaction, the resulting precipitate was collected by filtration, washed and finally calcined at 400 °C in a muffle furnace for 12 h.

Characterization

X-ray diffraction (XRD) patterns were obtained by an Empyrean Multi-Purpose Research X-Ray Diffractometer XRD by PANalytical with Cu K α radiation (0.15418 nm). Scanning electron microscopy (SEM) analysis was made with a Quanta 3D FEG Environmental Scanning Electron Microscope and Focused Ion Beam. For Raman spectroscopy and FTIR studies, a MicroRaman, Jobin Yvon-Horiba Labram 800 was used. The UV-Vis absorption spectra of the samples were obtained by diffuse reflectance studies using a Varian Cary model 100 spectrophotometer.

Photocatalytic activity evaluation

A 500 ml Pyrex glass vessel was used as a reactor in all experiments. Stirring was carried out with a PTFE coated

magnetic bar and a stirring plate. Air was introduced into the reaction solution from a compressor. The temperature of the photoreactor was held constant at 25 °C. The photocatalytic degradation of 4-chlorophenol in water was performed as following: 200 ml of an aqueous solution of 4-chlorophenol (80 ppm) was placed into the reactor in the presence of 200 mg of the ZnO catalyst. Air generated by an electric pump was bubbled into the solution at a rate flow of $1 \text{ ml} \cdot \text{s}^{-1}$. Then the mixed reaction solution was exposed to irradiation with a UV lamp that was made using a high pressure Hg pen-lamp (with irradiation of 254 nm and intensity of 2.2 mW/cm^2) encapsulated in a quartz tube immersed in the water solution for 6 hours. Aliquots (3 ml) were taken from the irradiated solution at different time intervals in order to follow 4-chlorophenol degradation. The 4-chlorophenol evolution was evaluated by using an UV-Vis spectrophotometer Cary 100 following the intensity of absorption band at $\sim 280 \text{ nm}$.

Results and discussion

FTIR spectra of the ZnO samples obtained by the three synthetic methods are shown in Figure 1. ZnO prepared by precipitation method shows a broad IR band at 3493 cm^{-1} with a low intensity which is assigned to the vibration mode of hydroxyls in adsorbed water (Figure 1a). The small band at 1628 cm^{-1} is assigned to the bending vibration of OH group in water. These observations confirm the presence of a small amount of water adsorbed onto the ZnO nanocrystal surface. Three strong and sharp bands at 1100 cm^{-1} , 880 cm^{-1} and 690 cm^{-1} are attributed to the vibrations of O-Zn bonds (Chelikowsky, 1977). The FTIR spectra of the samples obtained by UV irradiation and hydrothermal methods are shown in Figures 1b and 1c, respectively. Three IR vibrational bands are observed at similar position as for the ZnO obtained by precipitation method. However, the intensities of the IR bands in these two samples are much lower in comparison with that shown in the sample obtained by precipitation method.

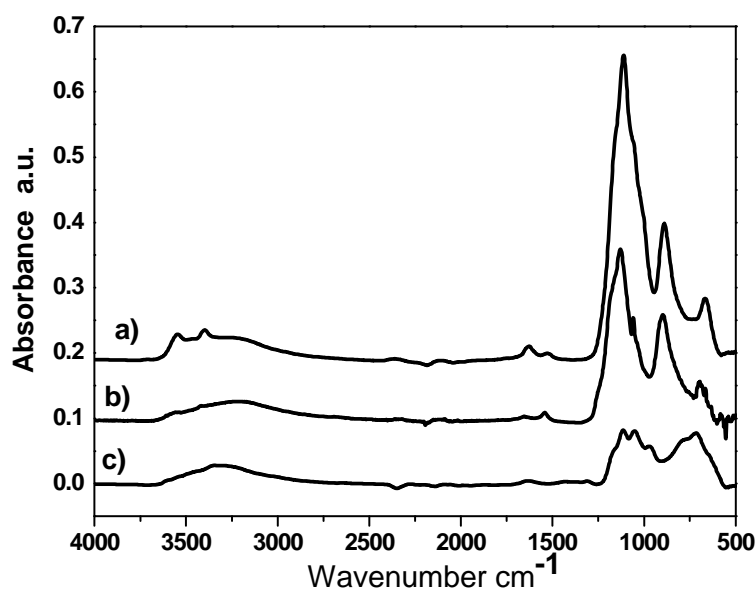


Figure 1. FTIR spectra of ZnO synthesized by different methods
a) Precipitation; b) UV irradiation and c) hydrothermal

The XRD patterns, Figure 2, confirm the formation of crystalline ZnO. The samples have a hexagonal phase with space group symmetry $P6_3mc$ (C_43v). The diffraction peaks correspond to a single phase with hexagonal wurtzite type described by the reflections of the crystal planes of (100), (102), (110), (103), (112) and (002). These results are in agreement with those reported in the literature (Yin et al., 2011; Rössler, 1969). The most intense peak is assigned to the reflection of the plane (002) in all samples. This reveals a preferential growth along the direction (002) in the ZnO crystals. The ZnO crystals grow along with their c axis perpendicular to the surface of the substrate, and thereby alters the crystallographic arrangement of the crystal (McCluskey et al., 2009). This direction of crystal growth is densely packed and the most thermodynamically favorable in a wurtzite structure. The intense signals can be clearly seen for the ZnO obtained by the precipitation method, Figure 2a; while for ZnO obtained by UV irradiation, the XRD peaks are less intense (see Figure 2b). The XRD patterns of the ZnO prepared by hydrothermal synthesis have the lowest intensities with sharp peaks among the three samples, indicating the larger particle size of this sample.

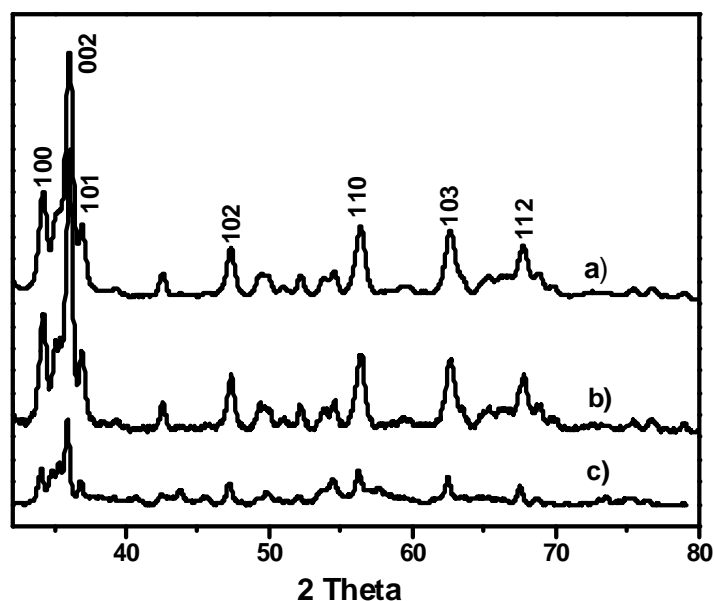


Figure 2. XRD patterns of ZnO synthesized by different methods. a) precipitation; b) UV irradiation; c) hydrothermal

Figure 3 shows the Raman spectra of the ZnO samples. According to the group theory (Poplewski et al, 2010; Wang 2011), vibration modes can be generally determined by $\Gamma_1 = A_1 E_1 E_2 A_1 A_2 + 2E + 2B_2 + E_2^3$, where A_1 , E_1 , and E_2 (E_2 (low), E_2 (high)) are Raman active modes (Shan, 2012). The polar characteristics of the vibration modes A_1 and E_1 carry longitudinal and transverse components designated as A_1 (TO), A_1 (LO), E_1 (TO) and E_1 (LO). In Figure 3, these vibrational modes are found at 103, 164, 197, 305, 419, 435 and 481 cm^{-1} . The band at 103 cm^{-1} mode is associated with E_2 (low), which corresponds to vibrations of the Zn sub-network. Mode E_2 (high) with high frequency locates at 435 cm^{-1} , corresponding to the typical sub-network of oxygen; it is also characteristic of the material attributed to an optical phonon non polar wurtzite phase of ZnO in the Raman active. The ZnO Raman peaks are well defined in the sample obtained by precipitation method, while the sample obtained by UV irradiation shows only three strong peaks at 103, 164 and 419 cm^{-1} ; this is associated with mode E_2 (low), which is related with vibrations of the Zn sub-network (Hammad et al., 2009; Nakahara et al., 2002; Arguello, 1969). It is note worthy that the band at 435 cm^{-1} that corresponds to the sub-network of lattice oxygen was not clearly observed in the samples synthesized by hydrothermal and was rather weak in the UV irradiation methods. This indicates that there exists oxygen deficiency or oxygen defects in the crystalline structure of these two solids.

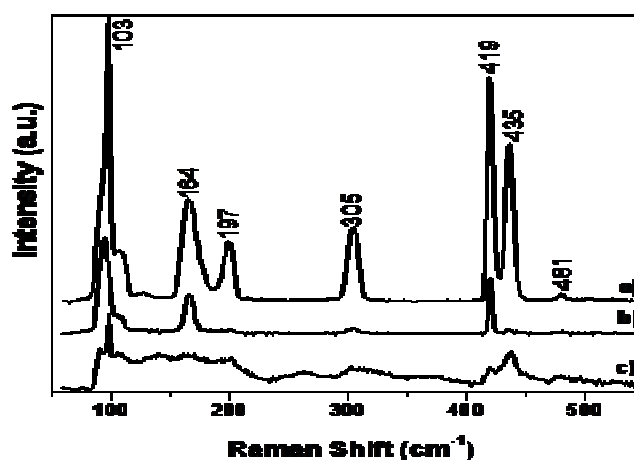


Figure 3. Raman spectra of ZnO synthesized by different methods a) Precipitation; b) UV irradiation; c) hydrothermal

The UV-Vis absorption spectra of ZnO nanostructures are shown in Figure 4. The band position at 375 nm (3.5 eV) and 230 nm (5.5 eV) correspond to Zn-O bonds in ZnO nanoparticles. With a strong UV-emission centered at 375 nm (3.5 eV), the ZnO synthesized by precipitation route preferentially orients in the [002] direction and has good crystallinity in the sample. ZnO is known to be an indirect semi conductor, therefore, a plot of the modified Kubelka–Munk function $[F(R\infty)E]^{1/2}$ versus the energy of the absorbed light E gives the band gap energies (Di Stefano, 2010; Su et al., 2010; Rossi et al., 1995; Hsueh et al., 2007). An example of determination of such values for the three ZnO samples is given in Figure 4. The energy of the band can be determined according to the following formula.

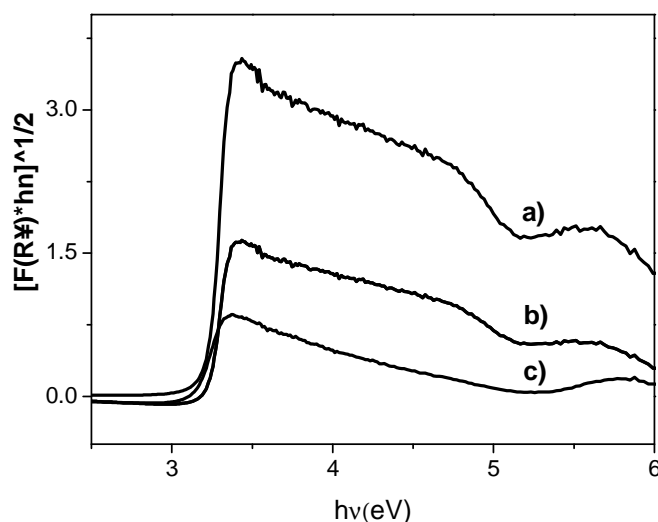


Figure 4. UV-vis spectra of ZnO synthesized by different methods. a) precipitation; b) UV irradiation; c) hydrothermal

$$\lambda = hc/E_{gap} = 1240/E_{gap} \quad (1)$$

where E_{gap} is the band gap energy in eV. The band gap energies obtained are 3.20, 3.31 and 3.31 eV for the ZnO obtained by precipitation, UV irradiation and hydrothermal methods, respectively. Obviously, the band gap energy of the ZnO sold obtained by precipitation route is the lowest among the three samples.

Different morphologies of the ZnO samples are observed by SEM. Nanorods in the ZnO synthesized with precipitation method can be observed in Figure 5a and 5b respectively. These rods have average value of diameters and lengths of approximately 1.6 and 1.2 microns. Figure 5b shows some cavities on the surface of the rods. During the preparation procedure, $Zn(OH)_2$ continuously produces Zn^{2+} and OH^- ions which form the ZnO nuclei that are the building blocks for the formation of the ZnO crystals. As the deposition over the ZnO nuclei increases in the unit-direction, the hexagonal-shaped ZnO nanorods are finally formed (Velmurugan, 2011; Wang et al., 2008). SEM micrographs for ZnO obtained by UV-vis irradiation synthesis route are presented in Figures 5c and 5d. Many thin layers with sharp boards are disorderd stacked around the nanoparticles. SEM micrographs of ZnO obtained by hydrothermal method are shown in Figures 5e and 5f. A large-scale flower-like morphologies are observed. The overall microstructures have an average size of 84 microns in diameter. Each individual flower-like structure is composed of many particles having diameters ranging from 8.1 to 9.7 microns. Some micro structures that make up the flower-like morphologies have a central area with an average diameter of 2.35 microns.

Photocatalytic degradation of 4-chlorophenol was carried out to evaluate the photocatalytic performance of ZnO obtained by the methods used herein. Figure 6 shows the variation of the UV-vis absorption spectra of 4-chlorophenol molecules as a function of degradation time. In the photodegradation process, the 4-chlorophenol molecules are first adsorbed on the ZnO surface. Next, the photo-excited electrons transfer from the solar light sensitize 4-chlorophenol molecule to the conduction band of ZnO, subsequently improving the electron transferring to the adsorbed oxygen (Egelhaaf, 1996), as described in the schematic model in Figure 7. Upon excitation of a photon with sufficient energy, electron-hole pairs are created, and the electrons may jump up to the conduction band. The separated electrons are capable of reducing an acceptor molecule, and the holes can oxidize the donor molecules. Electron-hole pair recombination takes place after the optically excited electrons lose energy through radiative and nonradiative paths, and

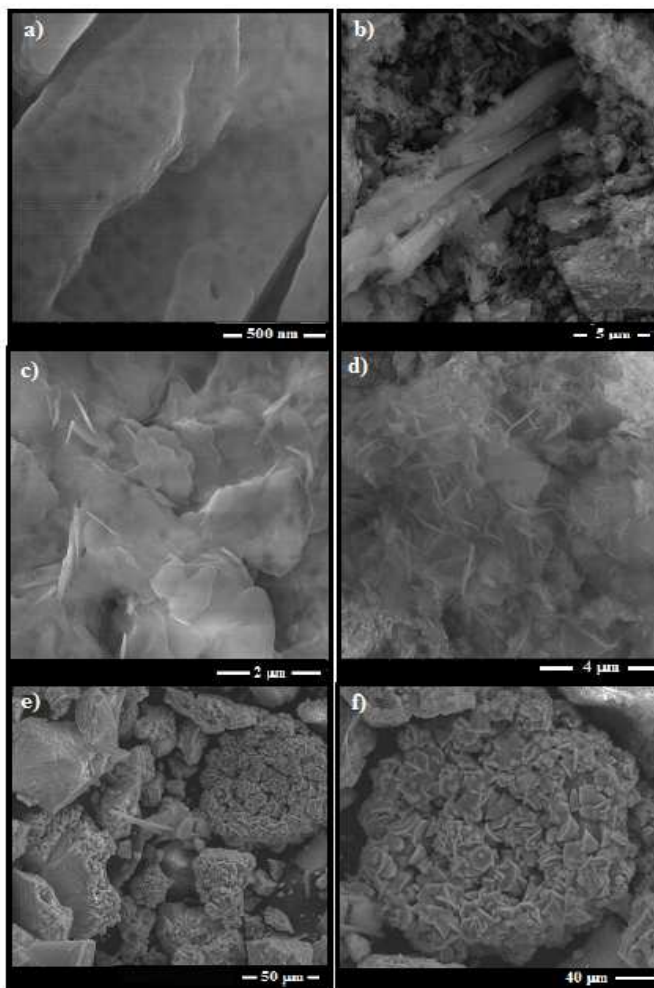


Figure 5. SEM images
 a) and b) of ZnO obtained by precipitation method.
 c) and d) of ZnO obtained by UV irradiation method.
 e) and f) SEM images of the ZnO obtained by hydrothermal method

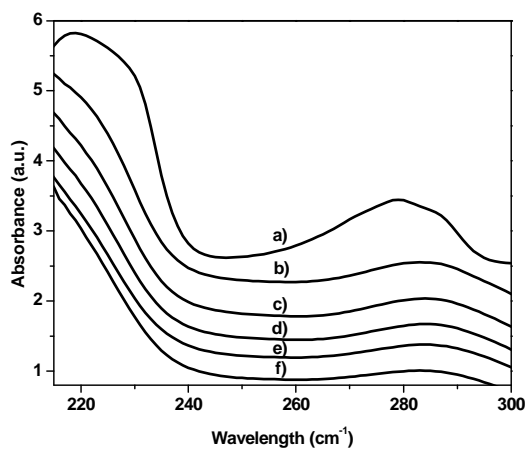


Figure 6. UV-vis spectra for the degradation of 4-chlorophenol after two hours of inder irradiation. a) t=0 min b)30 min c)60 min d) 90 min e)150min and f)180min

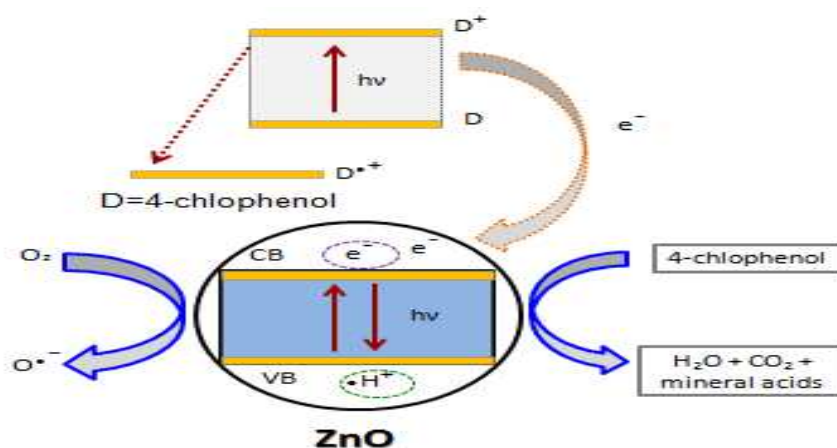
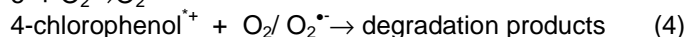
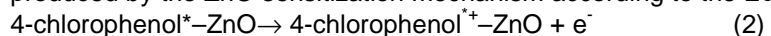


Figure 7. Schematic diagram for the transfer phenomena of an electron injected into ZnO

fall back to the valence band. The 4-chlorophenol molecules are photodegraded by the superoxide radicals ($O_2^{\bullet-}$) produced by the ZnO sensitization mechanism according to the Eqs. 2 to 4.



The time course of the 4-chlorophenol degradation was further studied. A plot of the relative concentration of 4-chlorophenol (C/C_0) as a function of irradiation time is depicted in Figure 8. The lowest activity of 4-chlorophenol degradation is observed using the ZnO sample obtained with hydrothermal method. Only 23% 4-chlorophenol are degraded (Figure 8a). In comparison with ZnO prepared by UV-Vis irradiation (Figure 8b) where 83% of 4-chlorophenol are degraded, the photodegradation of 4-chlorophenol is more efficient using ZnO nanorods prepared by the precipitation method (Figure 8c) where 99% of 4-chlorophenol are degraded after 150 min in UV irradiation under the same condition. These results indicate that the photocatalytic activity of ZnO appears to be correlated with the synthetic method. The sample obtained by precipitation method contains many ZnO nanorods with many vacancies on the surface. Because these vacancies can act as the active centers to capture photo-induced electrons, and the recombination of the electrons and holes can be effectively inhibited (Vanheusden et al., 1996; Auret et al., 2002; Faal Hamedani et al., 2006; Kim et al., 2007). In addition, the band gap energies of the ZnO crystals is 3.2 eV which is lower than that of the ZnO (3.31 eV) prepared with other two methods. Therefore, the photocatalytic activity of ZnO prepared by precipitation can be greatly promoted and much superior to that achieved in the other two samples.

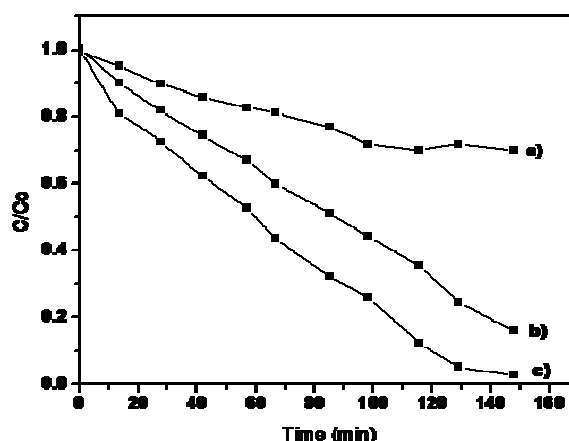


Figure 8. Evolution of photocatalytic degradation of 4-chlorophenol under UV radiation for the different preparation methods (a) hydrothermal; (b) UV irradiation; (c) precipitation method

It is note worthy that in the surfaces of the samples prepared by UV-Vis irradiation and hydrothermal methods, there exist a certain extent of structural oxygen deficiency, as indicated by Raman characterization. thisis unfavorable in the formation of surface active oxygen species Therefore, less number of active oxygen species like superoxide radicals ($O_2^{\bullet-}$) are generated during the photodegradation of 4-chlorophenol, which explains why the ZnO samples prepared by those two methods exhibit low photoactivity.

CONCLUSIONS

Using different synthesis methods, ZnO with different morphologies including flower-like, clusters and nanorods, were obtained. ZnO nanorods could be synthesized via precipitation method, while ZnO with flower-like structures could be synthesized by hydrothermal route. ZnO nanorods and flowers with wurtzite crystalline structure particularly grow along the [002] direction in all samples. The photocatalytic activity of ZnO appears to be correlated with the morphologies, band gap energy, and surface oxygen deficiency. The maximum activity for the photodegradation of 4-clorophenol under UV light irradiation was achieved on the ZnOnanorods with lower band gap energy synthesized by the precipitation method. Because of the higher band gap energy andsurface oxygen deficiency of the ZnO prepared by both UV-vis irradiation and hydrothermal methods is unfavorable in the formation of surface active oxygen species like superoxide radicals, these two samples exhibit lower photoactivity.

ACKNOWLEDGMENTS

The authors thank the technical support given by the Center of Nanoscience and Nanotechnology of the National Polytechnic Institute. Thanks also go to Dr. Micheal M. Timko at Worcester Polytechnic Institute for his kind comments in the manuscript modification.

References

- Agashe C, Kluth O, Schope G, Siekmann H, Hupkes J, Rech B(2002). Damp Heat Stable Doped Zinc Oxide Films. *Thin Solid Films*. 442: 167–172.
- AlmamunAshrafi ABM, Ueta A, Avramescu A, Kumano H, Suemune I, Ok YW, Seong TY(2000). Growth and characterization of hypothetical zinc-blende ZnO films on GaAs(001) substrates with ZnS buffer layers. *Appl. Phys. Lett.* 76: 550–552.
- Arguello CA, Rousseau DL, Porto SPS(1969). First-Order Raman Effect in Wurtzite-Type Crystals. *Phys. Rev.* 181: 1351–1363.
- Auret FD, Goodman SA, Legodi MJ, Meyer WE, Look DC(2002). Lasers Optics and Optoelectronics. *Appl. Phys. Lett.* 80: 1340–1346.
- Bates CH, White WB, Roy R(1962). New High-Pressure Polymorph of Zinc Oxide. *Science* 137: 993.
- Bunn CW(1935). The lattice-dimensions of zinc oxide. *Proc.Phys. Soc. London*, 47: 835–842.
- Chelikowsky JR(1977). An oxygen pseudopotential: Application to the electronic structure of ZnO. *Solid State Comm.* 22: 351–354.
- CRC (2005). Handbook of Chemistry and Physics, Lide, D. R. (ed.), 86th Ed., CRC Press, Boca Raton, FL. Pp. 2544.
- Di Stefano MC, Cabanillas ED, Trigubo AB, Rodríguez TC(2010). Tem Studies Of Zns Nanoparticles Obtained By Wet Chemical Reaction. *Acta Microscopica*. 19: 202–207.
- Dulub O, Boatner LA, Diebold U(2002). STM study of the geometric and electronic structure of ZnO(0001)-Zn, (000-1)-O, (10-10), and (11-20) surfaces. *Surf. Sci.* 519: 201–217.
- Dunliang J, Pu-Xian G, Wenjie C, Bamidele S, Allimi S, Pamir A, Yong D, Zhong LW, Christopher B(2009). Synthesis, characterization, and photocatalytic properties of ZnO/(La,Sr)CoO₃ composite nanorod arrays. *J. Mater. Chem.* 19: 970–975.
- Egelhaaf HJ, Oelkrug D(1996). Luminescence and nonradiative deactivation of excited states involving oxygen defect centers in polycrystalline ZnO. *J. Cryst. Growth*. 161: 190–194.
- Faal NH, Farzaneh F(2006). Synthesis Of Zno Nanocrystals With Hexagonal (Wurtzite) Structure In Water Using Microwave Irradiation. *Journal of Sciences, Islamic Republic of Iran*, 17(3): 231-234.
- Gerward L, Olsen JS(1995). The High-Pressure Phase of Zincite. *J. Synchrotron Radiat.* 2: 233–235.
- Gorrrn P, Rabe T, Kowalsky W, Galbrecht F, Scherf U(2006). Low loss contacts for organic semiconductor laser. *Appl. Phys. Lett.* 89: 161113.
- Hammad TM, Salem JK, Harrison RG(2009). Binding Agent Affect On The StructuralAnd Optical Properties Of Zno Nanoparticles. *rev. Adv. Mater. Sci.* 22: 74–80.
- Hsueh TJ, Hsu CL, Chang SJ, Lin YR, Chang SP, Chiou YZ, Lin TS, Chen IC(2007). Improved high-temperature characteristics of a symmetrically graded AlGaAs/In_xGa_{1-x}As/AiGaAs pHEMT. *IEEE Trans. Nanotech.* 6: 595-560.
- Jagannatha RA, Kokila MK, Nagabhushana H, Rao JL, Shivakumara C, Nagabhushana BM, Chakradhar RPS(2011). Combustion synthesis, characterization and Raman studies of ZnO nanopowder. *Spectrochimica Acta Part A*. 81: 53–58.
- Kim TW, Han AR, Hwang SJ, Choy JH(2007). Local Atomic Arrangement and Electronic Configuration of Nanocrystalline Zinc Oxide Hybridized with Redoxable 2D Lattice of Manganese Oxide. *J. Phys. Chem. C* 11: 16774-16780.
- Kogure T, Bando Y(1998). Formation of ZnO nanocrystallites on ZnS surfaces by electron beam irradiation. *J. Electron Microsc.* 47: 135–141.
- Liewhiran C, Phanichphant S(2007). Effects of Palladium Loading on the Response of a Thick Film Flame-made ZnO Gas Sensor for Detection of Ethanol Vapor. *Sensors* 7: 1159–1184.
- Look DC, Reynolds DC, Hemsley JW, Jones RL, Sizelove JR(1999). Production and Annealing of Elec- tron Irradiation Damage in ZnO. *Appl. Phys. Lett.* 75: 811–813.
- Maolin Z, Guoying S, Jiamo F, Taicheng A, Xinming W, Xiaohong H(2005). Novel preparation of nanosized ZnO–SnO₂ with high photocatalytic activity by homogeneous co-precipitation method. *Materials Letters*. 59: 3641-3644.

- McCluskey MD, Jokela SJ(2009). Defects in ZnO Applied. Review. *J. Appl. Phys.*106:071101: 1–13.
- Nakahara K, Takasua H, Fonsb P, Yamada A, Iwata K, Matsubara K, Hunger R, Niki S(2002). Growth of N-doped and Ga+N-codoped ZnO films by radical source molecular beam epitaxy. *J. Cryst. Growth*. Pp. 237–239, 503–508.
- Özgür Ü, Alivov YI, Liu C, Teke A, Reshchikov MA, Doğan S, Avrutin V, Cho SJ, Morkoç H(2005). A comprehensive review of ZnO materials and devices. *J. Appl. Phys.* 98: 1931–9401.
- Phillips JC(1973). Bonds and Bands in Semiconductors, Academic Press, New York..
- Poplewski G, Wałczyk K., Jeżowski J(2010). Optimization-based method for calculating water networks with user specified characteristics. *International J. Chem. Eng. Res.* 2: 109–117.
- Qamar M, Muneer MA(2009). A comparative photocatalytic activity of titanium dioxide and zinc oxide by investigating the degradation of vanillin. *Desalination* 249: 535–540.
- Rossi A, Tournèbeze A, Boule P(1995). Phototransformation of chlorohydroquinone in aqueous solution. *J. Photochem. Photobiol. A: Chem.* 85: 213–216.
- Rössler U(1969). A comparative photocatalytic activity of titanium dioxide and zinc oxide by investigating the degradation of vanillin. *Phys. Rev.B.* 148: 733–738.
- Shan G, Zheng S, Chen S, Chen Y, Liu Y(2012). Colloids and Surfaces B: Biointerfaces. 94: 157– 162.
- Soltani MA, Mahdy BS, Salehi H(2011). Density Functional Approach to Study Electronic Structure of ZnO Single Crystal. *World.J. Appl. Sci.* 10: 1530–1536.
- Su YK, Peng SM, Ji LW, Wu CZ, Cheng WB, Liu CH(2010). Ultraviolet ZnO Nanorod Photosensors. *Langmuir.* 26: 603–606.
- Suzan A, Khayyat MS, Akhtar AU(2012). ZnO nanocapsules for photocatalytic degradation of thionine. *Materials Letters.* 81: 239-241.
- Tsukazaki A, Ohtomo A, Onuma T, Ohtani M, Makino T, Smiya M, Ohtani K, Chichibu SF, Fuke S, Segawa Y, Ohno H, Koinuma K, Kawasaki M(2005). The lattice-dimensions of zinc oxide. *Nat. Mater.* 4: 42–45.
- Vanheusden K, Seager CH, Warren WL, Tallant DR, Voigt JA(1996). Correlation between photoluminescence and oxygen vacancies in ZnO phosphors. *Appl. Phys. Lett.* 68: 403–405.
- Velmurugan R, Swaminathan M(2011). An efficient nanostructured ZnO for dye sensitized degradation of Reactive Red 120 dye under solar light. *Sol.Ener. & Sol. Cells.* 95: 942–950.
- Wang HJ, Sun YY, Cao Y, Yu HX, Ji XM, Yang L(2011). Porous zinc oxide films: Controlled synthesis, cytotoxicity and photocatalytic activity. *J. Chem. Eng.* 178: 8–14.
- Wang Y, Li X, Wang N, Quan X, Chen Y(2008). Controllable synthesis of ZnO nanoflowers and their morphology-dependent photocatalytic activities. *Separation and Purification Technology.* 62: 727–732.
- Yin S, Goto T, Gobo F, Huang YF, Zhang PL, Sato T(2011). Phototransformation of chlorohydroquinone in aqueous solution Symposium. 2B: Novel Chemical Processing. Conf. Series: Materials Science and Engineering 18: 1-4.
- Yong D, Zhong LW(2007). Zinc-blende ZnO and its role in nucleating wurtzite tetrapods and twinned nanowires. *Appl. Phys. Lett.* 90: 153-510.